

## Superconductivity of Indium-Thallium Solid Solutions

J. W. STOUT AND LESTER GUTTMAN

*Institute for the Study of Metals, University of Chicago, Chicago, Illinois*

(Received July 28, 1952)

Measurements are reported on the superconducting properties of indium-thallium solid solutions in the composition range from pure indium to 50 percent thallium. The magnetic induction and the electrical resistance were measured at various temperatures and magnetic field strengths. Single crystal specimens of composition 0, 5, 10, 15, and 20 atom percent thallium, and polycrystalline specimens containing 15, 20, 38, and 50 percent thallium, were investigated. In the more dilute solutions the penetration of field into the specimen at constant temperature was sharp and the restoration of resistance occurred at substantially the same field. As the concentration of thallium increased, the flux penetration occurred over a wider range of field and the resistance appeared only after practically all the flux had penetrated. For the single crystal specimens the trapped flux in zero field was less than 20 percent of that corresponding to unit permeability at the field where flux penetration begins. The breadth of transition in the polycrystalline specimens was like that of the single crystals, but the trapped flux was much larger. The critical fields for destruction of superconductivity are given for the range 0 to 20 percent thallium and the electronic heat capacities of the normal metal are calculated from them.

PREVIOUS work on the superconducting properties of alloys<sup>1</sup> has indicated that, in contrast to the behavior of pure metals, alloy specimens are characterized by broad transitions extending over a range of temperature in zero magnetic field and, upon the application of a magnetic field at constant temperature, by a gradual penetration of flux into the sample occurring over a wide range of field strengths. Furthermore, the magnetic field necessary to restore electrical resistance is greater, often by as much as a factor of 10, than the field at which substantially all of the flux has penetrated into the specimen. Upon the removal of a magnetic field there is a large amount of trapped flux (absence of Meissner effect). These properties have been explained<sup>1</sup> by assuming that in an alloy there is a "sponge" structure so that different parts of a specimen have different critical temperatures and critical field strengths.

In an alloy consisting of two or more solid phases, one would expect that the physical and chemical inhomogeneities would account for a variation in superconducting properties throughout the specimen. However, for an ordered single-phase intermetallic compound there is no evident reason for inhomogeneities and indeed Shoenberg<sup>2</sup> has found that a carefully prepared specimen of the compound Au<sub>2</sub>Bi exhibits superconducting properties similar to those of a pure metal. In recent experiments on the compound MgTl we have found a similar behavior. In contrast to an ordered compound, a random solid solution is disordered on an atomic scale, but would be uniform on a scale comparable to the penetration depth of a magnetic field in a superconductor. In order to investigate the properties of a superconducting solid solution we chose the system indium-thallium. This system has the advantage that

the melting temperatures are convenient for growing single crystals and that the components are both ideal "soft" superconductors. Measurements of the transition temperatures of indium-thallium alloys made on polycrystalline specimens have been reported by Meissner, Franz, and Westerhoff.<sup>3</sup> By an x-ray investigation Guttman<sup>4</sup> has found that there is a continuous range of solid solutions extending from pure indium to 59 atom percent Tl. There is a transformation from a face-centered tetragonal to a face-centered cubic structure, at room temperature occurring at a composition of 22.7 atom percent thallium, but there is evidently no separation into two phases of different composition upon passing through this transition, which is probably one of second order.<sup>5</sup> Brief preliminary reports of our measurements on the superconductivity of indium-thallium alloys have been published.<sup>6</sup>

### PREPARATION OF SAMPLES

All samples used were in the form of cylinders about 6 mm in diameter and 15 cm long. Solutions of the appropriate composition were prepared by melting together pure indium (99.95 percent) and thallium (99.95 percent) with vigorous stirring under an atmosphere of nitrogen, and then casting in a cold graphite mold. The castings, which were about 19 mm in diameter, were rolled and swaged into cylinders. The single crystal samples were grown in precision bore Pyrex tubes into which the cylinders slipped easily. The inside of each tube was rinsed with a solution of 0.01 percent mineral oil in carbon tetrachloride. The thin film of oil

<sup>3</sup> Meissner, Franz, and Westerhoff, *Ann. Physik* [5] **13**, 505 (1932).

<sup>4</sup> L. Guttman, *J. Metals* (Trans. Am. Inst. Mining Met. Engrs. **188**, 1472 (1950)); Bowles, Barrett, and Guttman, *J. Metals* (Trans. Am. Inst. Mining Met. Engrs. **188**, 1478 (1950)).

<sup>5</sup> See J. W. Stout, *Phys. Rev.* **74**, 605 (1948).

<sup>6</sup> J. W. Stout and L. Guttman, *Phys. Rev.* **79**, 396 (1950); Proc. Natl. Bur. Standards Symposium on Low Temperature Physics (March, 1951) (unpublished).

<sup>1</sup> See, e.g., K. Mendelssohn, *Repts. Progr. Phys.* **10**, 358 (1946); D. Shoenberg, *Superconductivity* (Cambridge University Press, Cambridge, 1938), Chap. VI.

<sup>2</sup> D. Shoenberg, *Nature* **142**, 874 (1938).

TABLE I. Composition of In—Tl single crystal specimens.

Nominal	Atom percent thallium	
	Top	Bottom
5	5.04	5.05
10	10.07	10.07
15	14.91	15.26
20	19.35	20.43

remaining after the evaporation of the solvent facilitated the removal of the finished crystal. After insertion of the sample, the tube was evacuated to  $10^{-6}$  mm of mercury and sealed off. It was then placed in a vertical electric tube furnace controlled at such a temperature that the specimen was first entirely melted. The tube was then lowered at a rate of 13 mm per hour so that the solid grew from the bottom. The crystals could usually be removed from the tubes by gentle tapping, but in some cases, to avoid deformation, the glass was dissolved in HF solution without appreciably attacking the alloys. The samples as removed from the growing tubes were about 30 cm long. A region 15 cm long, of a single crystallographic orientation, was cut from each specimen by a glass string saw moistened with concentrated nitric acid. The saw cutting was entirely by the chemical action of the nitric acid, and the string pressure was not great enough to deform the single crystal. Etching with acetic acid and  $H_2O_2$  showed that the specimens employed for the superconductivity measurements were essentially single crystals, although some had small regions where slip had occurred in handling. The 20 percent thallium specimen had transformed from cubic to tetragonal during cooling to room temperature after solidification and there were transformation markings on its surface resembling, but on a much larger scale, those described by Guttman<sup>4</sup> for polycrystalline samples. The sample was probably a single crystal when it solidified from the melt, but in passing through the transformation it broke down into a set of tetragonal crystals having fixed orientations (see Bowles *et al.*<sup>4</sup>) relative to the original cubic axes. The energy of the interfaces between these various orientations of the tetragonal crystals, as is the case with boundaries between crystallographic twins, is apparently very small compared to that of ordinary grain boundaries in a polycrystalline specimen and we observed nothing in the superconducting properties of the 20 percent single crystal which could be ascribed to these boundaries.

Samples for analysis were taken from the regions near the cut ends of the specimen. The results are listed in Table I. The 5 and 10 percent specimens are uniform within the accuracy of the analysis, but the other two are definitely richer in thallium at the bottom end. Reference to the phase diagram<sup>4</sup> shows that at the melting point solid of 5 and 10 percent composition is in equilibrium with liquid richer in thallium, whereas the 15 and 20 percent solid is in equilibrium with indium

rich liquid. In the growing of a long single crystal, if there is no convection in the liquid, a steady state will be obtained in which the solid crystallizing has the over-all composition. The adjacent liquid is in equilibrium with this solid and there is a concentration gradient from the solid interface to a point beyond which the liquid has substantially the over-all composition. When the liquid in equilibrium with the solid is more dense (thallium rich) the region of concentration gradient is stable against convection; however, in the case of the 15 and 20 percent specimens convection probably occurred and a steady state was not attained.

In order to compare the behavior of single and polycrystal specimens and also to extend the composition range beyond the point where single crystals can be grown from the melt, a series of polycrystal specimens was prepared. To produce large grains, a strain-anneal technique was used. The cast samples were reduced to rods slightly larger than the desired final diameter and stretched in a tensile machine so as to obtain a uniform elongation of 2 to 3 percent. They were then cut to length, the ends rounded in a lathe, and the samples annealed in  $N_2$ -filled tubes in an oil bath at 140–145°C

TABLE II. Composition of In—Tl polycrystal specimens.

Nominal	Atom percent thallium	
	Top	Bottom
15	15.05	15.08
20	19.95	19.96
30	30.10	30.04
38	37.92	37.96
50	49.82	49.54

for 7–16 days. For the 50 percent specimen, the temperature was 118°C, obtained by boiling *n*-butyl alcohol. During annealing the individual crystals grew to a size of about 1 to 2 mm. The samples prepared by this technique were quite uniform in composition. The results of analysis of samples cut from the top and bottom of each specimen are shown in Table II.

#### APPARATUS

Measurements were made on all the specimens both of magnetic induction and electrical resistance at various temperatures and magnetic field strengths. A uniform magnetic field, parallel to the cylindrical axis of the samples, was provided by a solenoid mounted in the liquid nitrogen both surrounding the helium dewar. The solenoid was made of No. 16 Formex insulated copper wire wound in accurately turned grooves in four concentric Micarta tubes. The precision of the machining was such that the field for a given current could be calculated to within 0.1 percent from the dimensions of the solenoid. The magnetic field at the end of a 15-cm long specimen was 1.6 percent less than at its center and the variation over a region 4 cm long near the

center, the part which most influences the secondary coils, was only 0.1 percent.

For the induction measurements the samples were mounted in Lucite holders on each of which was wound a two-layer coil, 16 mm long, of about 300 turns of No. 40 Formex insulated copper wire. The Lucite tubes were machined to a thickness of 0.25 mm beneath the coils in order to minimize leakage flux. Slots were cut in the tubes to insure contact between the samples and the helium bath. Five specimen holders could be mounted in the Dewar, arranged symmetrically around a central tube which housed the stirrer for the bath, a Micarta screw driven by a variable speed motor. The specimen holders fitted accurately into a support which aligned the axis of the samples parallel to the field direction. The coils on the sample holders were connected through a selector switch to a ballistic galvanometer. In making a measurement the magnetic field in the solenoid was changed rapidly and the galvanometer deflection corresponding to the change in flux of induction through a coil was observed.

For the resistance measurements the samples were mounted in the Dewar in the same position relative to the solenoid as for the induction measurements. Current and potential leads were attached by means of small split copper rings held in place by brass screws kept tight with spring washers of phosphor bronze. The upper current lead was mounted rigidly on a Micarta support, but the other three leads were attached firmly only to the specimen so that no strain was produced by differential thermal contraction of the specimens and holder. There was negligible contact resistance at all temperatures between the specimens and the split rings to which the current and potential leads were soldered (with non-superconducting zinc-cadmium solder). No error was introduced because of possible contact resistance, since it enters into the resistance calculation only in its effect on the galvanometer sensitivity. The current (measured across a standard 0.01-ohm resistor) and the potential were read on a Wenner potentiometer with a sensitivity of about 0.01 microvolt. Because of the large size of the specimens the resistances of the samples were small, ranging at the boiling point of helium from  $1.53 \times 10^{-6}$  ohm for the pure indium to  $1.69 \times 10^{-4}$  ohm for the 50 percent thallium specimen. The accuracy of the resistance measurements was about 3 percent for the pure indium specimen and about 0.5 percent for the others.

The temperature of the samples was determined from the vapor pressure of the helium bath, using the table of van Dijk and Shoenberg.<sup>7</sup> At the higher pressures the bath pressure was held constant by a solenoid valve controlled by a mercury manometer and at the lower pressures was either controlled manually or allowed to come to equilibrium with the pump. In all measurements above the lambda-point the stirrer was operated

<sup>7</sup> H. van Dijk and D. Shoenberg, *Nature* **164**, 151 (1949).

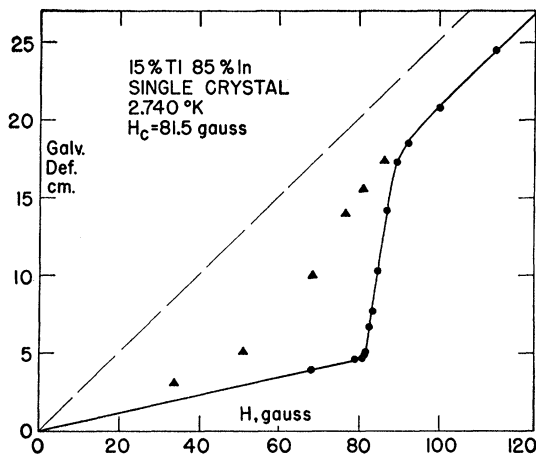


FIG. 1. Galvanometer deflection versus magnetic field.

to assist in obtaining temperature equilibrium throughout the bath. The resistance-temperature data in zero field were taken with the bath slowly cooling, since the temperature equilibrium is then assisted by convection. Warming curves gave apparent temperatures a few thousandths of a degree higher for the superconducting transitions, probably due to incomplete thermal equilibrium even in the stirred bath.

#### THE INDUCTION MEASUREMENTS

A typical set of data obtained in the measurement of the magnetic induction of a specimen at constant temperature and in different magnetic fields is shown in Fig. 1. In making a measurement the galvanometer deflection was observed corresponding to a sudden change of the applied magnetic field from some constant value to zero. The current in the solenoid was regulated by an electronic controller operating on the field current of the generator and could be set and held constant to better than 0.1 percent. The galvanometer deflection is proportional to the change in the flux of induction through the measuring coil surrounding the sample in going from a field equal to the solenoid field plus the earth's field to the earth's field alone. The value of the earth's field (0.4 gauss) was measured at the position of the samples, and a small correction has been made for this in the calculation of the magnetic induction in the sample. The dashed line in Fig. 1 is the curve for a sample of unit permeability, determined from measurements above the superconducting transition temperature. The points indicated by filled circles are obtained by setting the field at a constant value, approached from low fields, and then quickly switching it off. When the sample is completely superconducting, the small galvanometer deflections observed, due to the leakage flux between the sample and the coil, lie on a straight line through the origin. As the magnetic field is increased beyond a critical value, the flux penetrates into the sample with a rapid increase in galvanometer deflection.

TABLE III. Data on single crystal specimens from induction measurements.

Nominal composition percent thallium	Parameters for Eq. (1)			Observed data			
	$H_0$ gauss	$T_0$ , °K	$\gamma \times 10^4$ cal deg <sup>-2</sup> (g atom) <sup>-1</sup>	$T$ , °K	$B_0$ gauss	$H_c$ gauss	$H_c$ (obs)- $H_c$ (Eq. 1)
0	284.3	3.374	4.3	3.185	1.6	32.8	1.8
				2.975	3.8	63.9	0.6
				2.738	9.2	95.7	-1.4
				2.578	9.6	116.7	-1.6
				2.222	14.5	159.9	-1.1
				1.895	19.2	194.8	0.2
				1.325	25.9	242.1	1.7
5	276.5	3.280	4.3	3.170	3.1	20.5	2.3
				2.975	8.2	48.8	-0.2
				2.737	11.9	83.1	-0.9
				2.579	19.8	103.5	-2.1
				2.226	29.3	148.5	-0.7
				1.907	34.7	183.2	0.2
				1.309	42.8	233.9	1.4
10	284.7	3.255	4.6	3.162	2.7	17.8	1.7
				2.954	7.5	49.9	-0.3
				2.740	16.1	82.7	-0.3
				2.579	15.1	104.0	-2.0
				2.228	30.2	150.4	-0.9
				1.915	36.4	187.2	1.0
				1.301	48.5	239.9	0.7
15	281.1	3.252	4.5	3.152	2.3	16.0	-1.0
				2.946	8.2	50.4	0.0
				2.740	22.0	81.5	0.0
				2.591	17.6	104.2	1.5
				1.920	35.7	183.0	-0.1
				1.293	46.3	236.1	-0.6
				20	252.3	3.223	3.7
2.924	7.4	44.0	-0.6				
2.730	16.0	71.2	-0.1				
2.591	14.6	90.8	1.6				
1.922	21.1	164.2	1.6				
1.286	37.6	210.4	-1.7				

When the flux penetration into the sample is complete, ( $B=H$ ), the galvanometer deflections lie on a straight

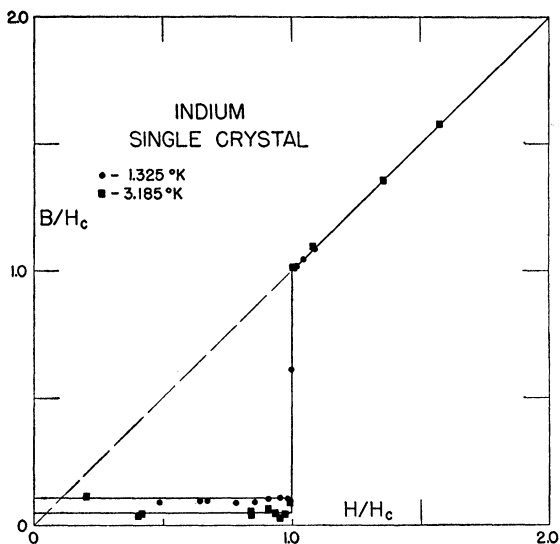


FIG. 2. Reduced magnetic induction versus reduced field.

line with slope equal to that observed for a sample of unit permeability, but displaced downwards by an amount proportional to the trapped magnetic induction,  $B_0$ , in zero field. Once a sample had been exposed to a field large enough to insure complete flux penetration, it was found that, at constant temperature, the value of  $B_0$  remained the same. This is indicated by the fact that at high fields the points for galvanometer deflection versus field lie on a straight line and by the reproducibility of the measurements. It was also found that the total flux change observed in decreasing the field to zero in several steps was equal to that of a single step over the same range of field, and that the galvanometer deflection in throwing a field off was equal to that observed when the same field was thrown on. The points indicated by triangles in Fig. 1 were obtained by first throwing on a large field at which flux penetration

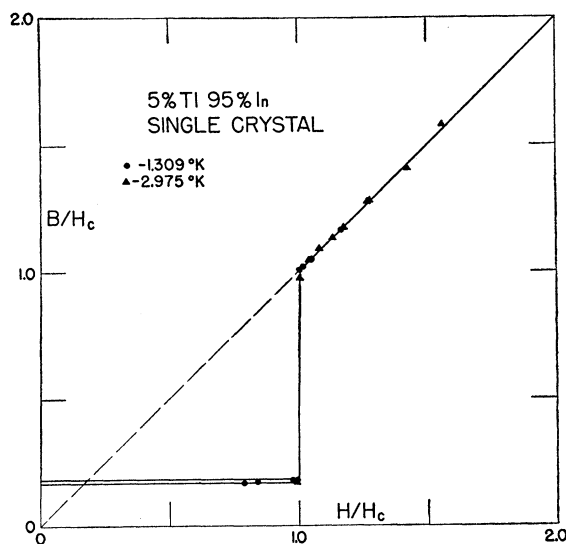


FIG. 3. Reduced magnetic induction versus reduced field.

is complete, decreasing the field to the value corresponding to the abscissa of the point, and measuring the galvanometer deflection when the latter field was reduced to zero. These points are evidence of a hysteresis in the induction in the sample according to whether a given value of field is approached from the high or low side. This type of hysteresis was found for the pure indium sample as well as the others. After some measurements had been taken on the indium single crystal with the roughly square ends left by the string saw, we removed the sample and rounded the ends by electrolytic polishing. This treatment considerably reduced the hysteresis observed on reducing the field, but did not otherwise change the curve of galvanometer deflection versus field. In Table III the data at 2.738 and 2.222°K are for the specimen with the ends rounded.

Since, when the fields were approached from the low

side, the shape of the curves for the pure indium specimens and the more dilute alloys corresponded to the sharp penetration of flux at a critical field characteristic of an ideal superconductor, most of our measurements were made in this fashion. In the curves given below, the hysteresis points have been omitted and the plotted points represent the flux of induction, as approached from low fields, in samples previously conditioned by exposure to a supercritical field and then brought back to zero field. If one calls  $\Delta$  the observed galvanometer deflection *versus* field above the superconducting transition temperature, and  $k_2$  the slope of galvanometer deflection *versus* field when the sample is completely superconducting, then the change in induction in the sample upon changing from field  $H$  to zero is given by

$$B - B_0 = (\Delta - k_2 H) / (k_1 - k_2).$$

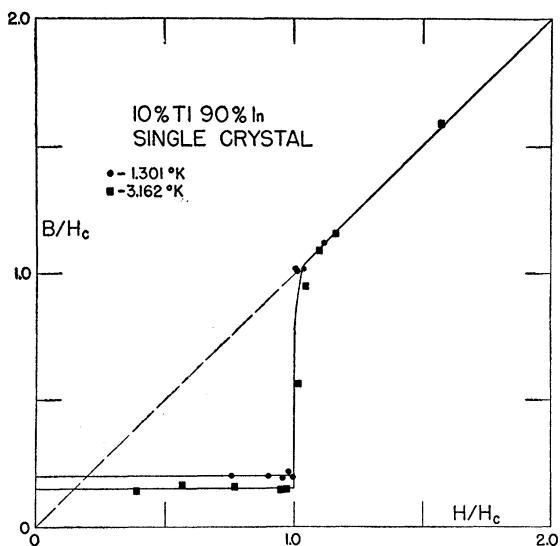


FIG. 4. Reduced magnetic induction *versus* reduced field.

The points at high fields when  $B = H$  serve to determine the value of  $B_0$ . In the case of the single crystal specimens we found that the beginning of flux penetration occurred sharply, and although in the 15 and 20 percent specimens measurements taken very close together in field showed a slight rounding rather than an abrupt discontinuity at the start of flux penetration, it was easy to choose a critical field as the intersection, on a plot of galvanometer deflection *versus* field, of the straight line corresponding to the completely superconducting region with the rapidly rising curve corresponding to the penetration of flux. Wexler and Corak<sup>8</sup> have found that when flux penetration occurs over a range of field, the field corresponding to initial flux penetration corresponds most closely to the thermodynamic critical field. The values of the critical fields,  $H_c$ , and of the residual induction in zero field,  $B_0$ , are

<sup>8</sup> A. Wexler and W. C. Corak, Phys. Rev. **85**, 85 (1952).

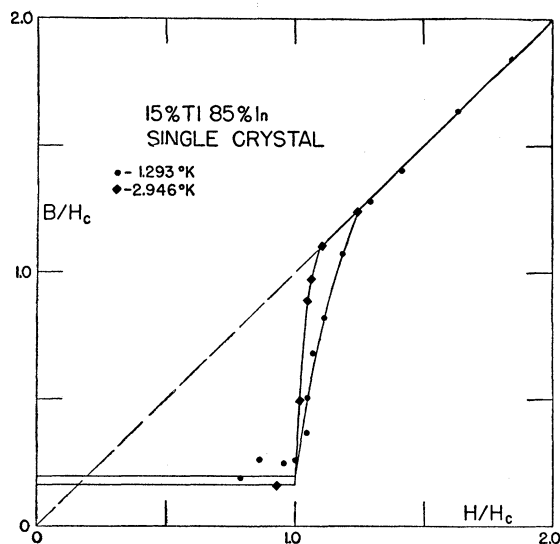


FIG. 5. Reduced magnetic induction *versus* reduced field.

given in Table III. The observed critical fields fitted fairly well the parabolic expression

$$H_c = H_0(1 - T^2/T_0^2). \quad (1)$$

The values of the parameters  $H_0$  and  $T_0$  for each composition are listed in Table III and the deviations of the observed critical fields from those calculated by Eq. (1) are given.

In Figs. 2 to 6 are plotted the values of  $B/H_c$  *versus*  $H/H_c$  for the five single crystal specimens. In order to avoid a clutter of indistinguishable points, we have included for each sample only data at a relatively high and a relatively low temperature. In general, the curves at the other temperatures listed in Table III fall between those shown on the graphs. For the pure

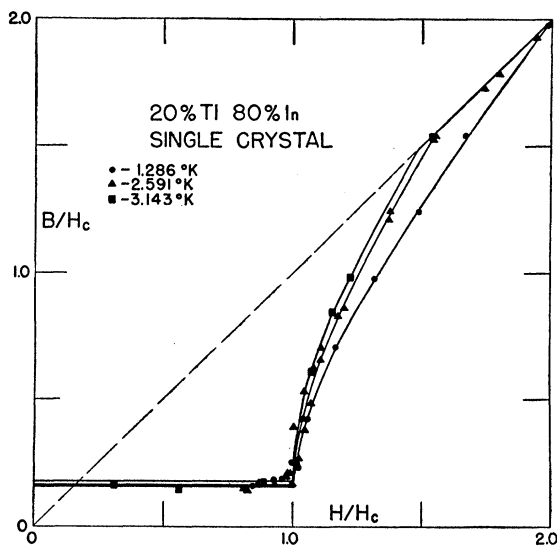
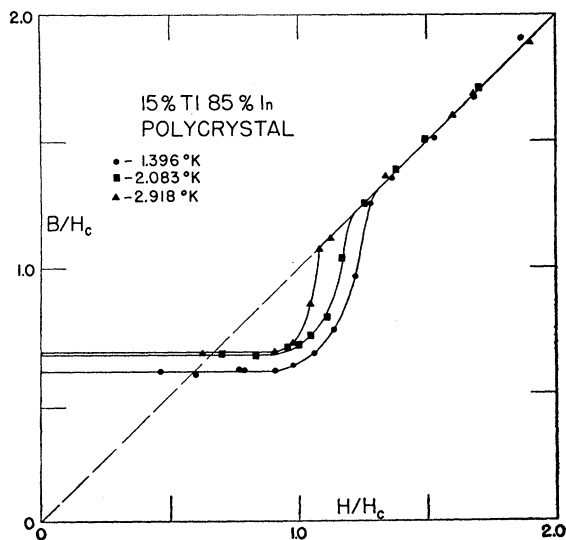
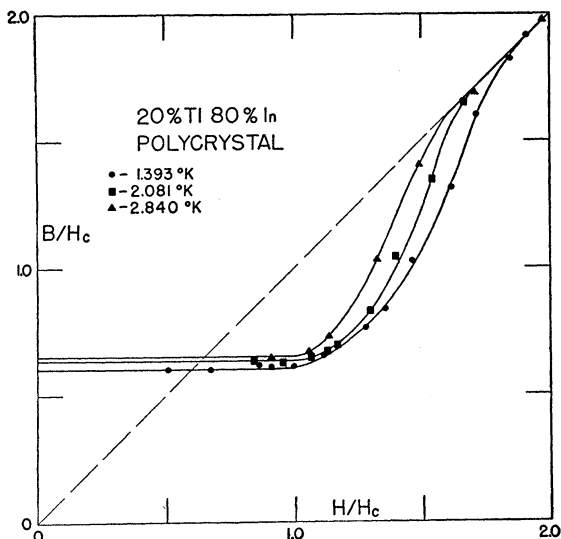
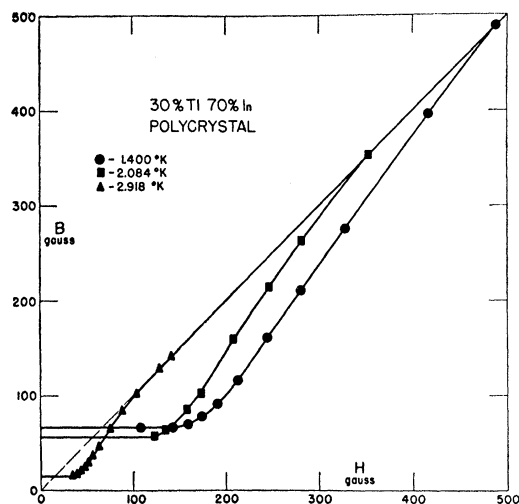


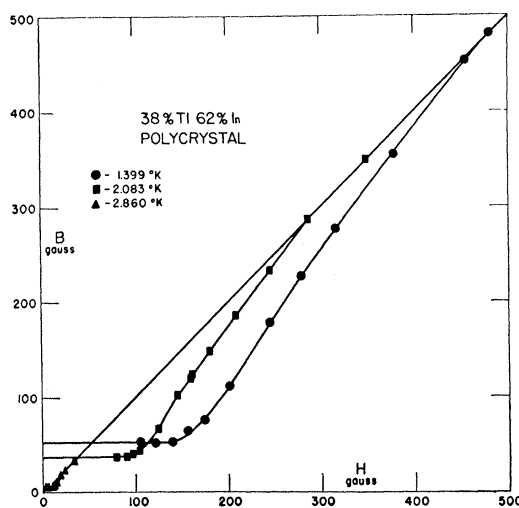
FIG. 6. Reduced magnetic induction *versus* reduced field.

FIG. 7. Reduced magnetic induction *versus* reduced field.

indium and the 5 and 10 percent thallium samples the shape of the curve of  $B/H_c$  *versus*  $H/H_c$  was within the limits of error the same at all temperatures. The transitions are quite sharp. For the indium and the 5 percent alloy, the flux penetration was complete within less than 1 percent range of field. For the 10 percent sample the initial flux penetration was rapid, but there is some rounding at the high field side, indicating that a field about 4 percent greater than the critical field is necessary to obtain substantially complete flux penetration. The curves for various temperatures superimposed within the accuracy of the measurements. The 15 and 20 percent specimens showed an increasing range of flux penetration and for these specimens the range was broader at lower temperatures, as can be seen by refer-

FIG. 8. Reduced magnetic induction *versus* reduced field.FIG. 9. Magnetic induction *versus* magnetic field.

ence to Figs. 5 and 6. At the lowest temperature a field of  $1.25 H_c$  for the 15 percent and  $2 H_c$  for the 20 percent was needed to obtain nearly complete flux penetration. A further set of induction measurements was made on the 20 percent single crystal specimen quenched from a high temperature. For this experiment the sample was held at a temperature of  $110^\circ\text{C}$  for three hours in an inert atmosphere and then quickly transferred to a bath of liquid nitrogen. In 55 seconds it had cooled to the boiling point of nitrogen and was then quickly transferred to the helium bath and the induction measurements taken. It was thought possible that in the slow cooling of specimens, as was previously done, there might be a beginning of separation into phases stable at lower temperatures and that the width of transition might be due to this effect. However, the induction curves in the quenched specimen were very similar to

FIG. 10. Magnetic induction *versus* magnetic field.

those shown in Fig. 6. X-ray diffraction measurements made at liquid nitrogen temperatures show no evidence of phases other than the face-centered tetragonal one for the 20 percent composition.

The results of induction measurements on 15 and 20 percent polycrystalline specimens are shown in Figs. 7 and 8. The critical fields used in calculating  $B/H_c$  and  $H/H_c$  are those obtained from measurements on the single crystal specimens of the same composition. In general, the over-all breadth of the transition for the polycrystalline specimens is similar to that for the single crystals; however, the trapped flux in zero field is very much larger and the initial penetration gradual, so that it would be very difficult to define a critical field from these curves alone. In Figs. 9, 10, and 11 are shown the magnetic induction,  $B$ , plotted against field for the 30,

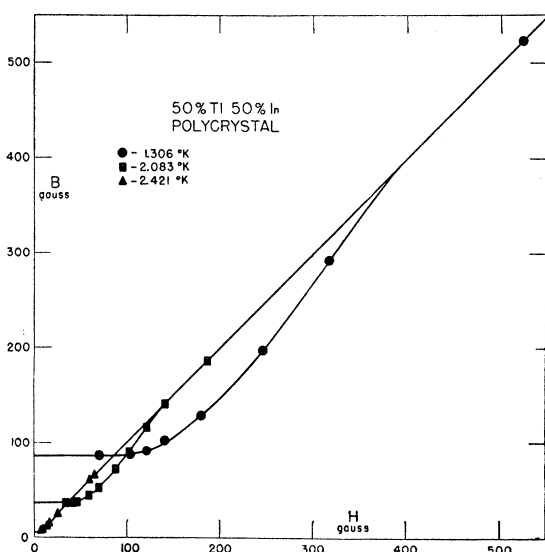


FIG. 11. Magnetic induction *versus* magnetic field.

38, and 50 percent polycrystalline specimens. In these samples there is as much as a factor of 3 between the field strengths when flux penetration begins and is complete. Because of the gradual initial penetration of flux, it was not possible to choose a critical field with any precision and the data are consequently not given in terms of  $B/H_c$  and  $H/H_c$ . There is no great variation in the width of transition or shape of the curves in these three samples.

#### THE RESISTANCE MEASUREMENTS

These measurements were made on the same samples as were used for the induction measurements. The resistance-temperature curves for the single crystal specimens are shown in Fig. 12 and for the polycrystalline specimens in Figs. 13 and 14. These curves were all taken with slow cooling in the earth's magnetic field (0.4 gauss) and the observed data have been corrected to zero field. The measuring currents used are indicated

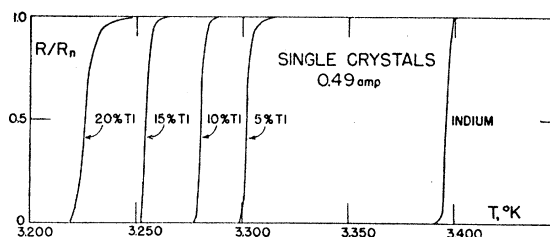


FIG. 12. Reduced resistance *versus* temperature.

on the figures. The ordinate on the plots is the ratio of the observed resistance,  $R$ , to the resistance,  $R_n$ , when the sample is completely nonsuperconducting. During a cooling curve the samples were under continuous observation, and the curves drawn represent a large number of points all lying on the curve. A few measurements, indicated as points, were taken for the polycrystalline specimens at different measuring currents. These points, which are definitely not on the curve, show a decrease in apparent transition temperature with larger measuring currents. The effects are larger by factors of 20 to 100 than would be calculated from Silsbee's hypothesis.

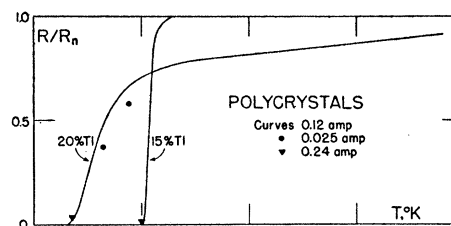


FIG. 13. Reduced resistance *versus* temperature.

The transitions for the single crystal specimens are all quite sharp, and although there is a gradual increase in breadth in going from the pure indium to the 20 percent specimen, even for the latter the major drop in resistance occurs within  $0.01^\circ$ . The polycrystalline 15 percent specimen has a transition curve practically identical with the single crystalline one. The polycrystalline 20 percent specimen begins to acquire resistance at the same temperature as the single crystal, but the curve is much broader and has a very long high temperature tail. The transitions in the 30 and 38 percent polycrystalline specimens occur over a range

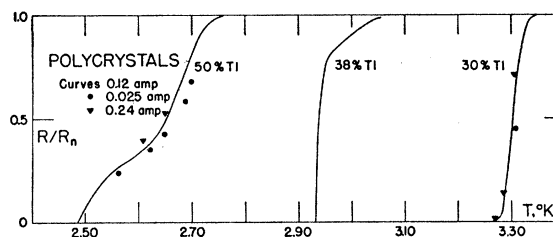


FIG. 14. Reduced resistance *versus* temperature.

TABLE IV. Temperature at which  $R/R_n=0.5$ .

Single crystals		Polycrystals	
Nominal composition percent Tl	$T$ , °K	Nominal composition percent Tl	$T$ , °K
0	3.396	15	3.254
5	3.302	20	3.233
10	3.280	30	3.304
15	3.254	38	2.938
20	3.226	50	2.652

of temperature of about  $0.1^\circ$ . The wide transition curve covering about  $0.25^\circ$  and the unusual shape of the curve for the 50 percent sample may be because in this specimen the stable room temperature structure was formed by a reaction in the solid state between face-centered and body-centered cubic phases rather than directly by crystallization from the melt.<sup>4</sup> Although no evidence of two phases was found by metallographic examination of the annealed sample, nor was any indicated by the induction measurements, an extremely small amount of a different phase might affect the resistance measurements, which are sensitive to traces of superconducting impurities.

The zero field transition temperatures for the single crystal specimens obtained from extrapolation of the induction data agree within the accuracy of the extrapolation (about  $0.01^\circ$ ) with those observed in the resistance measurements. The values of  $T_0$  given in Table III agree less well because a quadratic function does not adequately represent the induction data. The temperatures corresponding to the restoration of half the normal resistance are given in Table IV and represented graphically in Fig. 15. For comparison, the data of Meissner, Franz, and Westerhoff<sup>3</sup> on polycrystalline

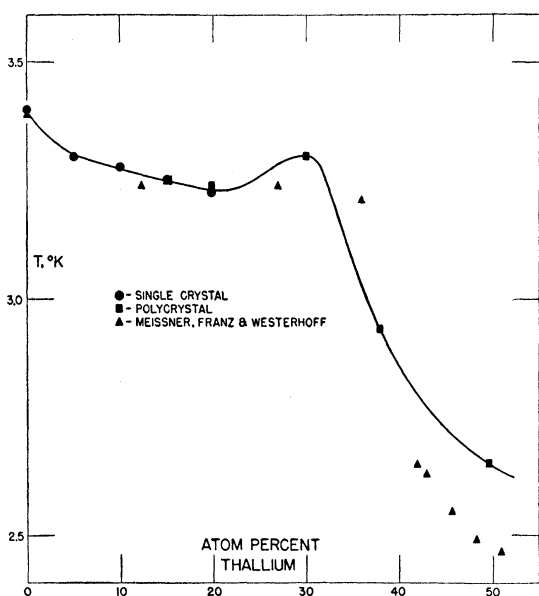


FIG. 15. Transition temperature in zero field versus composition.

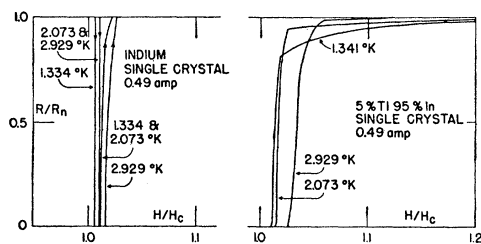


FIG. 16. Reduced resistance versus reduced field.

specimens are shown. From measurements of the electrical resistance at higher temperatures reported elsewhere<sup>9</sup> we believe that at the temperatures of liquid helium the specimens ranging in composition from indium through 30 percent thallium have a face-centered tetragonal structure, whereas the 38 and 50 percent compositions are face-centered cubic. The rapid drop in

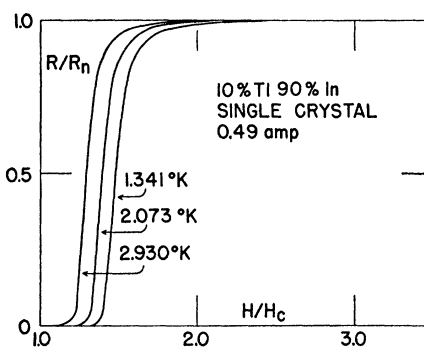


FIG. 17. Reduced resistance versus reduced field.

transition temperature that begins between our 30 and 38 percent samples may be related to this fact.

The restoration of electrical resistance upon the application of an external magnetic field is shown in Figs. 16-19 for the single crystal specimens and in Figs. 20-24 for the polycrystal ones. For the specimens up to 20 percent thallium the fraction of the resistance in the normal state is plotted against the reduced field,

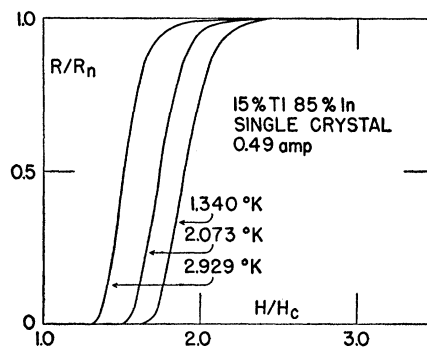


FIG. 18. Reduced resistance versus reduced field.

<sup>9</sup> J. W. Stout and L. Guttman, Phys. Rev. 88, 713 (1952).

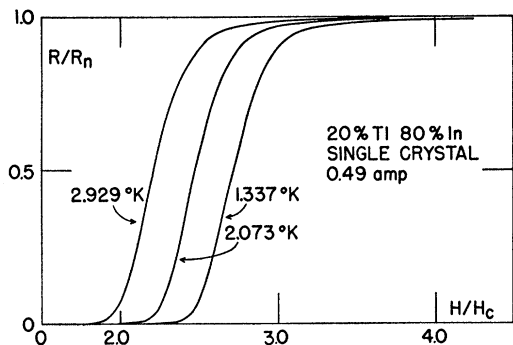


FIG. 19. Reduced resistance versus reduced field.

$H/H_c$ , where the appropriate critical field was calculated from the induction measurements on the single crystal specimens. In the case of the 30, 38, and 50 percent specimens where the critical field could not be accurately estimated, we have plotted the fractional resistance against the measured field. For all samples measurements were made with both increasing and

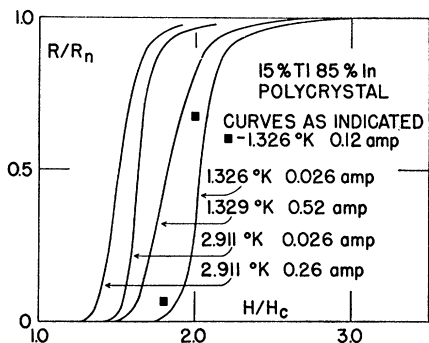


FIG. 20. Reduced resistance versus reduced field.

decreasing field. For the pure indium the resistance is restored sharply at a field 1 to 2 percent larger than the critical field for flux penetration. A slight hysteresis of about 1 percent in field was observed in the pure indium sample between the increasing field at which the normal resistance was restored and the decreasing field at which the resistance suddenly dropped to zero. Within the

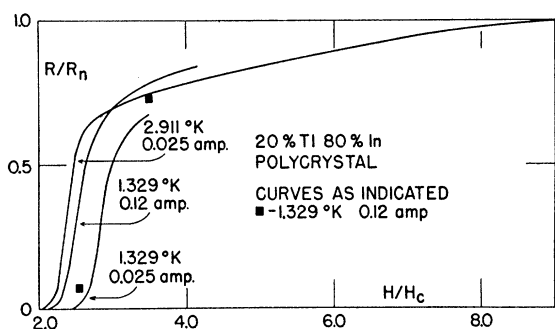


FIG. 21. Reduced resistance versus reduced field.

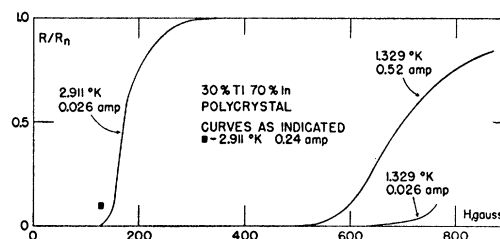


FIG. 22. Reduced resistance versus field.

accuracy of the measurements there was no hysteresis in the other samples.

The restoration of resistance in the 5 percent single crystal occurred at a value of  $H/H_c$  comparable with that for pure indium except at the highest temperature where a field about 3 percent greater than  $H_c$  was required. The curves for the 10, 15, and 20 percent single crystal specimens show increasing breadth of transition and increasing values of  $H/H_c$  for a given restoration of resistance as the amount of thallium in the alloy increases. In these specimens the value of  $H/H_c$  to obtain a certain restoration of resistance

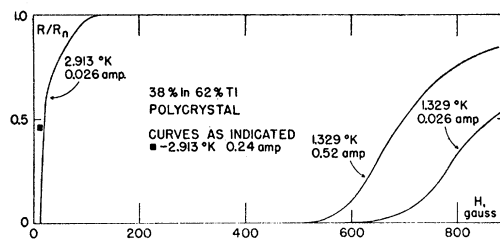


FIG. 23. Reduced resistance versus field.

increases as the temperature is lowered. The polycrystalline specimens containing 15 and 20 percent thallium show curves resembling those of the single crystal specimens, except that there is a break and a long tail on the high resistance side for the 20 percent sample. This high resistance tail was also noted in the resistance-temperature data in zero field for the same specimen; the reason for it is not clear. In the polycrystalline specimens several measuring currents were used and it was found that increasing measuring current appreciably reduced the field necessary to restore a given fraction of the normal resistance. Each curve

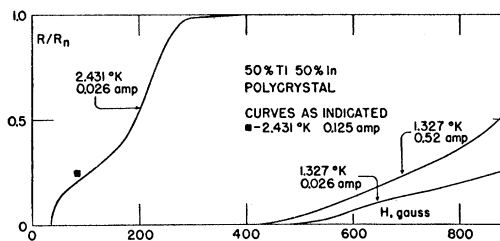


FIG. 24. Reduced resistance versus field.

shown represents many points which are not indicated. When only a few measurements were taken at a certain current, they are shown as separate points and the corresponding curve is not drawn. In the 30, 38, and 50 percent polycrystalline specimens the restoration of resistance begins at a magnetic field comparable to that at which flux penetration was found in the induction measurements to be substantially complete, and extends over a wide range of field strengths. The curve for the 50 percent specimen reflects the behavior found for this specimen in the resistance-temperature data previously discussed.

### DISCUSSION

The measurements show that the single crystals resemble pure metals much more closely than has been found previously<sup>1</sup> for alloys. In particular, the field at which flux penetration begins is sharply defined, and most of the flux is expelled on decreasing the applied field to zero. As one goes from pure indium to 20 percent thallium the breadth of the region over which flux penetration occurs upon the isothermal application of a magnetic field gradually increases. The restoration of resistance begins at a field greater than that required for substantially complete flux penetration and is completed over a range of field which is greater the larger the thallium content of the sample. The effect of the addition of thallium on the superconducting properties is, however, much more gradual than the effect on the normal electrical resistivity at low temperatures.<sup>9</sup> Thus the addition of 5 percent thallium produces very little change in breadth of the superconducting transitions but increases the resistivity at the boiling point of helium by a factor of 16. In the single crystal specimens the trapped flux in zero field is 15 to 20 percent of the flux that would be present in a specimen of unit permeability at the field where penetration begins. If the field at which flux penetration begins is taken as the true critical fields, the samples exhibit therefore a Meissner effect of 80 percent or more. The breadth of the flux penetration *versus* magnetic field curves for polycrystalline specimens in which the crystals were grown in the solid state is similar to that for the single crystals; however, the polycrystalline specimens showed a much larger trapped flux, or smaller Meissner effect.

The increase of breadth of transition in a magnetic field with increasing thallium content of the alloy appears to be a characteristic of the solid solution. Since, however, for the single crystal specimens the resistance transitions in zero field were quite sharp and to a first approximation the magnetic transition curve for a given concentration scales as the critical field, it appears that the breadth of transition is principally connected with the mechanism of the destruction of superconductivity by a magnetic field. Because of the finite penetration depth the field to destroy superconductivity is greater in a thin filament than in a bulk specimen. To explain the sharp transitions in a longitudinal magnetic field observed in pure metals, it is necessary to postulate a surface energy between the normal and superconducting regions which makes the formation of small superconducting filaments energetically unfavorable.<sup>10</sup> If the surface energy decreases with increasing thallium content in the alloys, one would expect a widening of the magnetic field transitions. In such a case the field at which flux penetration begins should correspond to the thermodynamic critical field, and when this point is sharply defined as it was in our single crystal specimens one may use the critical fields so obtained to deduce (using well-known thermodynamic formulas) the difference in entropy and heat capacity between the normal and the superconducting state. By assuming the parabolic relation (Eq. (1)) and with the further assumption that there is no term linear in temperature in the heat capacity of the superconducting state, one may calculate the electronic heat capacity of the normal metal. This heat capacity is given by  $C_n = \gamma T$ , where  $\gamma = VH_0^2/2\pi T_0^2$ . In making the calculation, the lattice parameters observed by Guttman<sup>4</sup> were used to calculate the gram-atomic volume  $V$ . The values of  $\gamma$  calculated from the values of  $H_0$  and  $T_0$  are given in Table III.

We are indebted to Mr. Stanley Reed for assistance in preparing the specimens and with the measurements, to Mr. K. K. Ikeuye for help in the growing of the polycrystalline specimens, and to the members of the analytical chemistry section for making the chemical analyses.

<sup>10</sup> F. London, *Superfluids* (John Wiley and Sons, Inc., New York, 1950), Vol. I, p. 125.